ACS Catalysis

pubs.acs.org/acscatalysis

Research Article

Tunable Aziridinium Ylide Reactivity: Noncovalent Interactions Enable Divergent Product Outcomes

Kate A. Nicastri, Soren A. Zappia, Jared C. Pratt, Julia M. Duncan, Ilia A. Guzei, Israel Fernández,* and Jennifer M. Schomaker*

Cite This: *ACS Catal.* 2022, 12, 1572−1580

Read Online

ACCESS | Metrics & More | Article Recommendations | Supporting Information

ABSTRACT: Methods for rapid preparation of densely functionalized and stereochemically complex *N*-heterocyclic scaffolds are in demand for exploring the potential bioactive chemical space. This work describes experimental and computational studies to better understand the features of aziridinium ylides as intermediates for the synthesis of highly substituted dehydromorpholines. The development of this chemistry has enabled the extension of aziridinium ylide chemistry to the concomitant formation of both a C−N and C−O bond in a manner that preserves stereochemical information embedded in the substrate. Additionally, we have uncovered several key insights that describe the importance of steric effects, rotational barriers around the C−N bond of the aziridinium ylide, and noncovalent interactions on the ultimate reaction outcome. These critical insights will assist in the development of this chemistry to generate *N*-heterocycles that will further expand the complex amine chemical space.

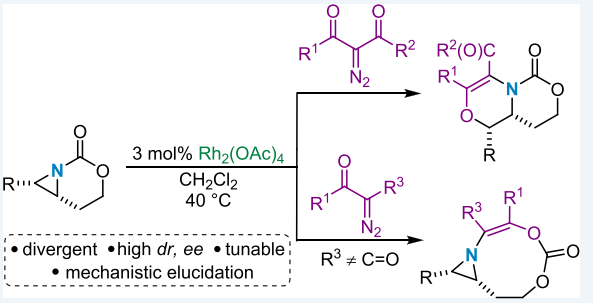

KEYWORDS: *aziridine, aziridinium ylide, carbene, morpholine, tunability, noncovalent interactions*

INTRODUCTION

Onium ylides,[1−5] including sulfur,[6a−d] oxonium,[7] and ammonium,[8a,b] are common intermediates employed in the syntheses of complex molecules. They are typically generated from the reaction of a heteroatom with a metal-supported carbene to furnish reactive zwitterionic intermediates that engage in a diverse set of reaction pathways, including 1,2-Stevens rearrangements,[8b] 2,3-sigmatropic rearrangements,[9] and N−H insertion reactions (Scheme 1A).[3] The aziridinium ylides[10] represent a unique subclass of ammonium ylides whose reactivity is both poorly understood and underexplored, despite the potential for these reactive species to serve as key intermediates in the transformation of simple precursors to densely functionalized, stereochemically rich *N*-heterocycles. We are interested in applying the ability to shuttle aziridinium ylides along divergent pathways to explore the diverse new amine chemical space, particularly in the context of using our new methods for the preparation of DNA-encoded libraries (DEL) to explore their potential bioactivity.[11a−c]

Manipulating the reactivity of aziridinium ylides to achieve a desired reaction outcome can be challenging as compared to their acyclic ammonium counterparts. Aziridinium ylides are embedded in a highly strained ring, where the bonding constraints of the aziridine increase the energy required for pyramidal inversion of the nitrogen; often, this rate is slow enough to measure using variable-temperature (VT) or dynamic NMR spectroscopy.[12a−c] The presence of two invertomers hinders the ability to selectively form and engage aziridinium ylides in secondary reactions and has limited their applications in the synthesis of complex *N*-heterocycles. For example, in 2001 and 2004, respectively, Clark et al.[13] and Rowlands[14] observed intramolecular [2,3]-Stevens rearrangements of aziridinium ylides to deliver dehydropiperidines in low 21−24% yields (Scheme 1B). In the former case, the low yield was attributed to the instability of the starting material, which decomposed in one day when stored under argon at −30 °C.[13] In Rowlands' work, the alkyl aziridine substrate existed as two *N*-invertomers **a** and **b** in a ratio of 3:4, with an estimated barrier to *N*-inversion at room temperature of ∼16−20 kcal/mol. Only **a** possessed the required geometry for the desired rearrangement; as a result, the major invertomer **b** underwent an unproductive 1,5-hydride shift at a faster rate than *N*-inversion to generate the invertomer required for the desired reactivity.[14] In addition to the formation of invertomers of the aziridinium ylide, competitive cheletropic extrusion renders the use of these intermediates in selective transformations particularly challenging.[15]

We used rigid bicyclic aziridines (Scheme 1C), generated by silver-catalyzed nitrene transfer of homoallenic and homoallylic

Received: November 25, 2021
Revised: December 23, 2021
Published: January 11, 2022

https://doi.org/10.1021/acscatal.1c05413
ACS Catal. 2022, 12, 1572−1580

Scheme 1. (A–D) Prior Work in Aziridinium Ylide Chemistry and New Divergent Reactivity

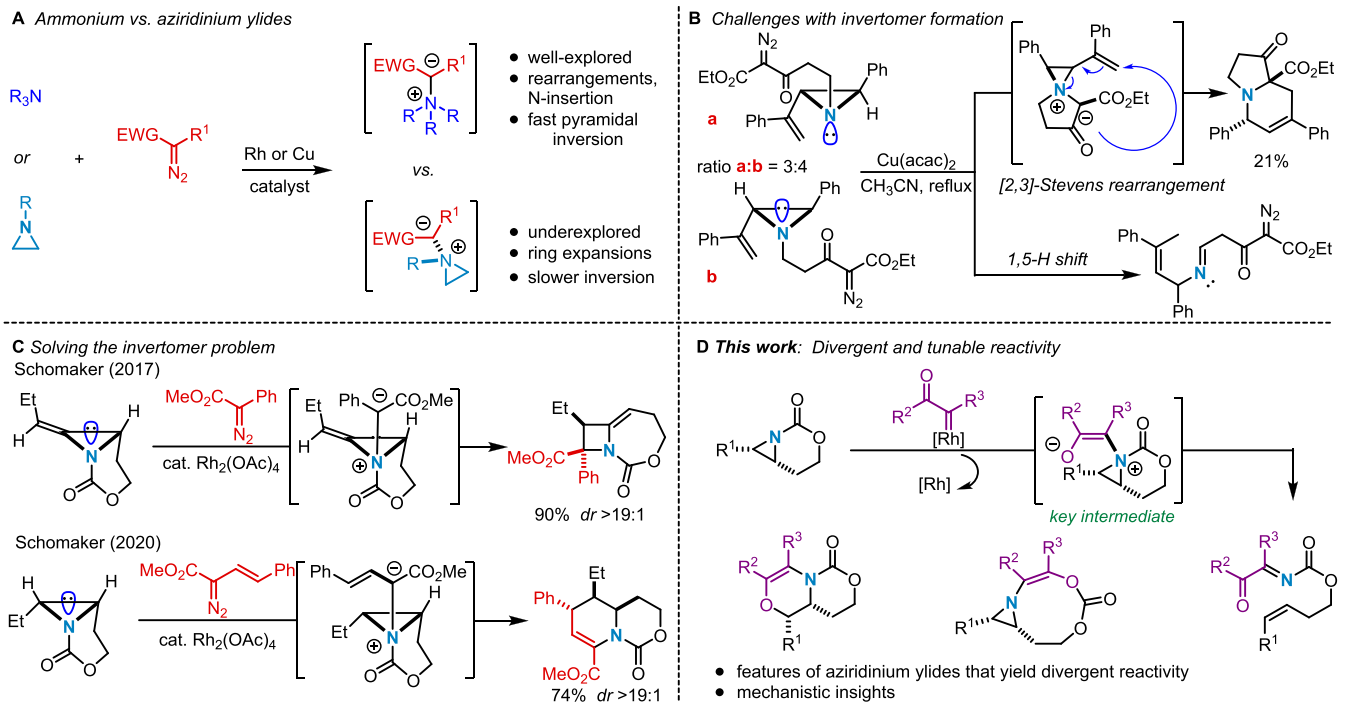

Scheme 2. (A,B) Ring Expansions of 1 with Diazoketone Carbene Precursors[a]

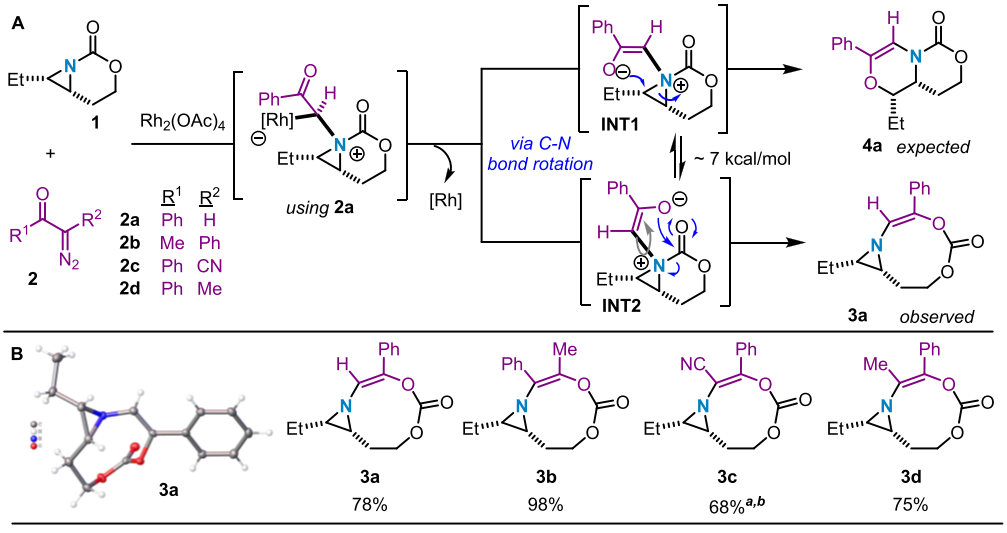

[a]Standard conditions: Slow addition of the diazoketone (3.0 equiv) over 3 h to a mixture of 3 mol % $Rh_2(OAc)_4$ and aziridine (1.0 equiv) in CH_2Cl_2 at 40 °C. Yields are given for isolated products. [a]Yields determined by ^1H NMR using 1,3,5-trimethoxybenzene as an internal standard. [b]A small amount of **4c** (19%) was also detected in this crude ^1H NMR spectrum.

carbamates, as precursors to aziridinium ylides.[16a−c] The nitrogen of the carbamate tether in the bicyclic aziridine possesses a hybridization of ~ sp^3, where the nitrogen lone pair is unable to engage in effective orbital overlap with the π system of the carbonyl group. As a result, the carbamate behaves as a σ-electron-withdrawing group and raises the barrier to *N*-pyramidal inversion.[17] The geometric constraint imposed by the bicyclic nature of the tether also raises the nitrogen inversion barrier;[17] a similar effect is observed in rigid cyclic amines such as sparteine and Tröger's base.[18a,18,19a,b] Both of these unique structural characteristics can be exploited to generate diastereomerically enriched aziridinium ylides that ultimately furnish highly substituted methyleneazetidines[20a,b] and dehydropiperidines[21] in an excellent yield and *dr* (Scheme 1C). This strategy effectively circumvents competing pathways that have been proposed in previous attempts to leverage the reactivity of aziridinium ylides. However, despite this progress, the future development of productive chemistry of aziridinium ylides requires a more detailed understanding of how the identity of the carbene precursor, potential dynamic behavior in the ylide intermediate, and noncovalent interactions influence the ultimate outcome of the reaction. In this work, we describe our mechanistic findings to explain divergent reaction pathways from aziridinium ylides generated by

https://doi.org/10.1021/acscatal.1c05413
ACS Catal. 2022, 12, 1572−1580

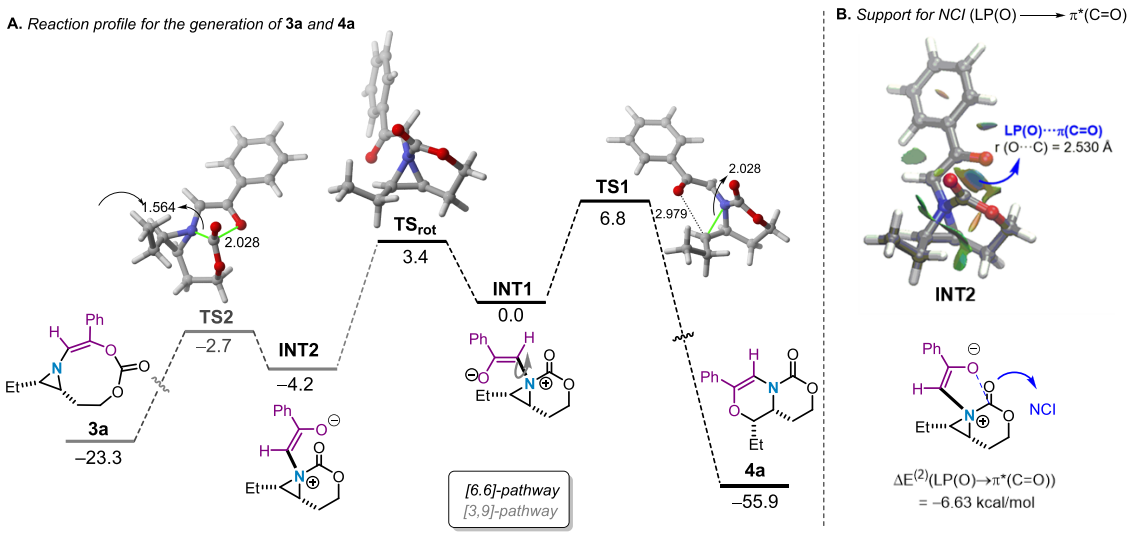

Figure 1. (A) Computed reaction energy profiles for formation of **3a** and **4a**. Relative free energies (ΔG_{298}, at 298 K) and bond distances are given in kcal/mol and angstroms, respectively. (B) Contour plots (left) of the reduced density gradient isosurfaces (density cutoff of 0.04 a.u.) for intermediate **INT2**. The green surfaces indicate attractive noncovalent interactions. Associated SOPT-NBO stabilizing energy (right). All data have been computed at the SMD(CH_2Cl_2)B3LYP-D3/def2-SVP level of theory.

leveraging ketone-containing carbenes, derived from Rh catalysis, to furnish fully substituted dehydromorpholines (Scheme 1D).[22−24] Both experimental and computational studies are presented that will inform future efforts of our and other groups' work on these fascinating and versatile reactive species.

RESULTS AND DISCUSSION

Initial Explorations of Diverse Carbene Precursors. We first investigated whether the carbonyl oxygen of an acceptor diazoketone, such as **2a**, could serve as a competent nucleophile to open the aziridinium ylide en route to a dehydromorpholine (Scheme 2A). Only one nucleophilic ketone group is present in **2a**; thus, we expected the reaction of **2a** with **1** to furnish **4a** in a good yield via the conformer **INT1**. Surprisingly, treatment of **1** with **2a** under $Rh_2(OAc)_4$ catalysis gave an unusual [3,9]-aziridine product **3a** in a 78% yield. Presumably, the 7 kcal/mol barrier to interconversion of aziridinium ylide **INT1** to **INT2** by rotation around the C−N bond (Scheme 2) enables nucleophilic attack of the ketone oxygen on the electrophilic carbonyl of the carbamate tether to furnish **3a**. This result was unexpected, as nucleophilic addition to the carbamate tether was not observed in previous syntheses of azetidines or dehydropiperidines from bicyclic aziridines.[20a,20,21]

We were curious as to the origin of **3a** and hypothesized that the aryl group may be important in biasing the reaction toward this unexpected product. However, exchanging the Ph group of **2a** to a Me group in **2b** still furnished **3b** in an excellent 98% yield (Scheme 2B). Altering the electronics of R^2 had no effect on product selectivity. Both electron-withdrawing and electron-donating substituents (e.g., CN in **2c** and Me in **2d**) furnished [3,9]-aziridine in 75 (**3d**) and 68% (**3c**) yields, respectively (Scheme 2B). The consistent product outcome suggested that neither R^1 nor R^2 influences the preferred formation of the [3,9]-aziridine product.

To gain more insight into the formation of **3a** at the expense of the expected **4a**, density functional theory (DFT) calculations were carried out at the dispersion-corrected SMD(CH_2Cl_2)-B3LYP-D3/def2-SVP level (see computational details in the Supporting Information). Figure 1A shows the computed reaction profiles leading to the formation of **3a** or **4a** from the corresponding free aziridinium ylides, which according to our previous calculations on related systems[20b,21] derives from the nucleophilic addition of the aziridine **2a** to the Rh_2-carbenoid intermediate (formed upon the reaction of the diazo compound and $Rh_2(OAc)_4$). From the data in Figure 1A, it becomes apparent that the metal-free ylide **INT2** involved in the [3,9]-pathway is lower in energy than its analogous intermediate **INT1** involved in the alternative [6,6]-pathway ($\Delta\Delta G$ = −4.2 kcal/mol). A similar finding was observed in their metal-ylide counterparts ($\Delta\Delta G$ = −5.7 kcal/mol). According to the NCIPLOT method, this is in part ascribed to the occurrence of a stabilizing NCI involving the nucleophilic C−O lone pair of the ketone moiety and the electrophilic π^*(C═O) molecular orbital of the carbamate, as confirmed for **INT2** (Figure 1B; see also Figure S-14 in the Supporting Information for the metal-ylide intermediate **INT2-Rh**). The presence of this stabilizing NCI is also supported by the computed short O···C(═O) distance in **INT2** of 2.530 Å, which is markedly shorter than the sum of the van der Waals radii (3.22 Å); this was also confirmed by the associated stabilization energy (ΔE^2 = −6.63 kcal/mol) computed for the lone pair (LP)(O)→π^*(C═O) interaction using the second-order perturbation theory (SOPT) of the NBO method (Figure 1B). Furthermore, the barrier associated with the formation of **3a** from **INT2** is 5.3 kcal/mol lower than that associated with the formation of **4a** from **INT1** (Figure 1A). This noticeable difference in the calculated activation energies for the two potential reaction pathways and the occurrence of the NCIs, which show significant stabilization of the key ylide intermediate, lead to the preferred formation of **3a** over **4a**, despite the fact that the latter species is significantly favored thermodynamically. The barrier to interconversion between **INT1** and **INT2** (7.6 kcal/mol, Figure 1A) is reinforced by the lower barrier ($\Delta G^{\neq}$ = 1.5 kcal/mol) computed for the generation of the observed product **3a**.

https://doi.org/10.1021/acscatal.1c05413
ACS Catal. 2022, 12, 1572−1580

Scheme 3. (A) Controlling Product Distribution Using Temperature, (B,C) Computed Reaction Profile (Relative Free Energies Are Given in kcal/mol) at the SMD(CH_2Cl_2)B3LYP-D3/def2-SVP Level at 25 and 83 °C (Values within Parentheses) and Contour Plots of the Reduced Density Gradient Isosurfaces (Density Cutoff of 0.04 a.u.) for the Intermediate INT4, and (D) Scope of the Process

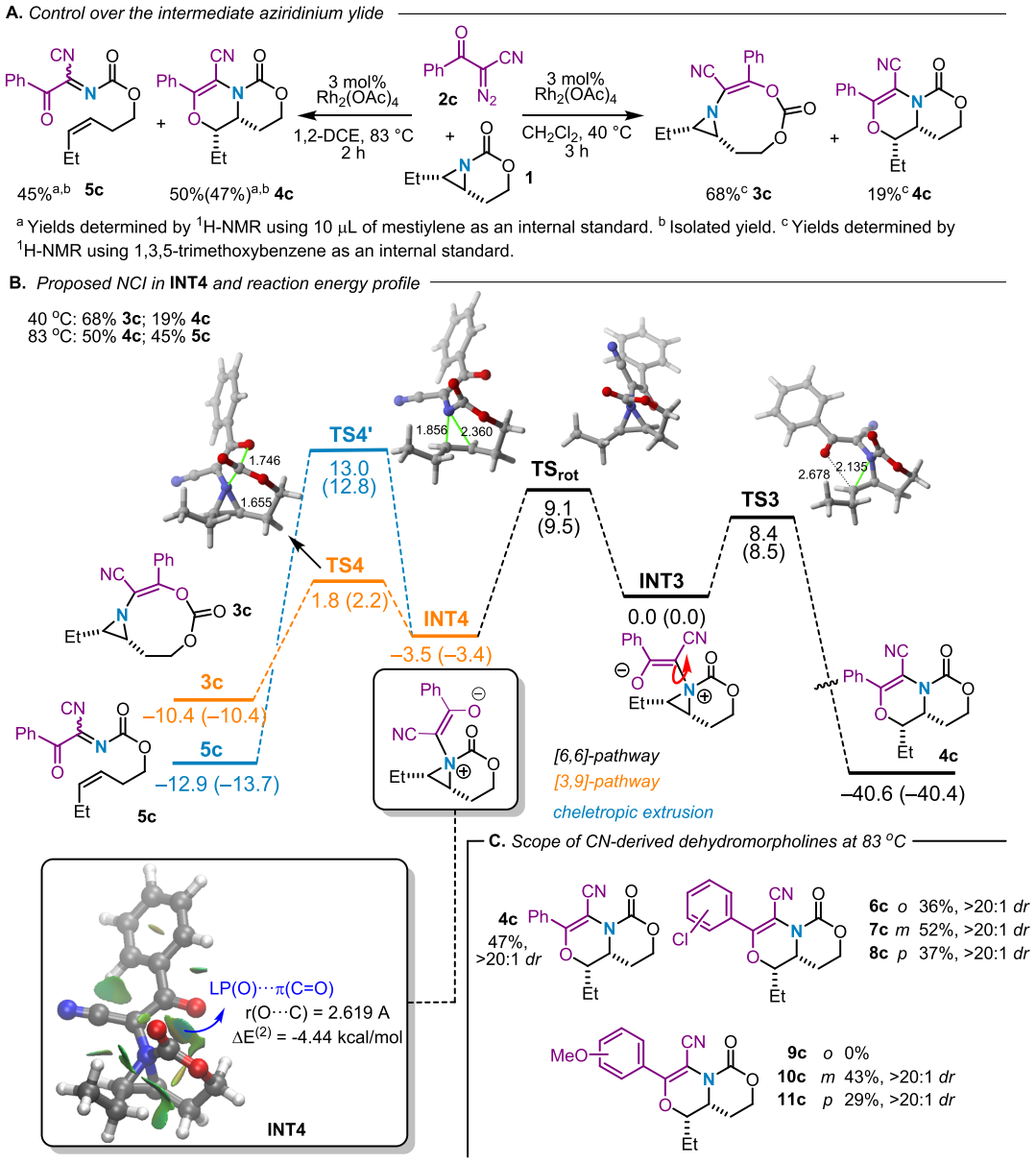

Controlling Product Outcomes with Temperature. Changing the carbene precursor to the CN-containing diazoketone **2c** provided the first example of divergence between dehydromorpholine **4c** and the [3,9]-aziridine **3c**. Standard reaction conditions furnished **3c** in a 68% yield (by NMR), accompanied by 19% of the dehydromorpholine **4c** (Scheme 3A, right). The 3.6:1 ratio of **3c**:**4c** led us to employ computations to probe whether an NCI was also present in the corresponding aziridinium ylide and to estimate the barrier to C–N bond rotation. Computational analysis confirmed the presence of an NCI, where the O···C(=O) distance of **INT4** is predicted to be 2.619 Å (Scheme 3B compared to 2.530 Å, Figure 1B), with a stabilizing interaction energy of ΔE^2 = −4.44 kcal/mol. The balance between the computed barrier to C–N bond rotation between **INT3** and **INT4** of 12.5 kcal/mol and the presence of an NCI lead to a divergent reaction where both **3c** and **4c** are accessible. These computational observations are reflected in the calculated reaction profile (Scheme 3B), where both the activation energy barriers leading to **3c** and **4c** are accessible ($\Delta G^{\neq}$ of ∼8.5 kcal/mol) but slightly higher than that of **3a** (Figure 1, see above). The higher barrier to C–N bond rotation (compared to the analogous ylide **INT2**) is likely a result of charge delocalization across the CN group (as compared to the ketone in **INT2**); nonetheless, it is still low enough to ultimately give rise to the product distribution based on temperature.

The computed reaction profile depicted in Scheme 3C also shows that the NCI-stabilized ylide **INT4** can undergo a cheletropic extrusion reaction to form the alkene **5c**. We hypothesized that running the reaction at higher temperatures would (i) enable facile bond rotation and lead to a greater preference for **4c** over the [3,9]-aziridine product **3c** and (ii)

https://doi.org/10.1021/acscatal.1c05413
ACS Catal. 2022, 12, 1572−1580

allow access to the cheletropic extrusion product. To our delight, repeating this reaction at 83 °C in 1,2-dichloroethane (Scheme 3A, left) favored dehydromorpholine **4c** formation in a 50% yield by ^{1}H NMR (47% isolated), with the remaining mass balance (45% yield) accounted for by formation of **5c**; no [3,9]-aziridine **3c** formation was observed. Although full selectivity for **4c** would be optimal, this reaction represents the first example where the fate of the aziridinium ylide can be controlled by the reaction conditions and not just the identity of the carbene precursor.

Employing higher temperatures with other cyano-derived diazoketones also proved fruitful (Scheme 3C). Ketones bearing *ortho*-, *meta*-, and *para*-chlorosubstituted benzenes yielded dehydromorpholines **6c**–**8c** in moderate yields and excellent *dr* of >20:1. Ketones with *meta*- and *para*-methoxysubstituted benzenes were tolerated to furnish dehydromorpholines **10c** and **11c** in 43 and 29% yields, respectively. The *ortho*-substituted **9c** was not observed under these conditions, possibly due to steric congestion around the reactive site that prevents effective ylide formation.

Based on our computational analysis of [3,9]-aziridine formation in Figure 1A, strategies to prohibit NCI formation in the key ylide intermediate were envisaged to promote formation of the desired dehydromorpholines. We hypothesized that increasing the barrier to C–N bond rotation in the aziridinium ylide intermediate could "trap" the kinetically formed conformer(s) and prevent formation of the NCI, potentially favoring a conformer similar to **INT1** (Scheme 1A). To this end, the barriers for C–N bond rotation in aziridinium ylides generated from the reaction of **1** with carbene precursors **2a** and **2d**–**f** were calculated and compared (Figure 2). The results suggest that aziridinium ylides arising from the reaction of **1** with **2a** (which experimentally gave [3,9]-aziridines **3a**, Scheme 1B) display a low barrier of ca. 7 kcal/mol to rotation about the C–N bond (black line). The reaction of **1** with **2d** revealed a higher barrier of 12 kcal/mol (green line) for C–N bond rotation. In contrast, aziridinium ylides formed from the reaction of **1** with dicarbonyl-containing diazo compounds **2e** and **2f** show significantly higher barriers to rotation around the C–N bond at ∼23 (red line) and 20 kcal/mol (blue line), respectively. The increased rotational barrier may be attributed to the ability of the enolate of the ylide to be delocalized over both carbonyl-containing groups, providing additional structural rigidity and steric bulk that hinders C–N bond rotation.

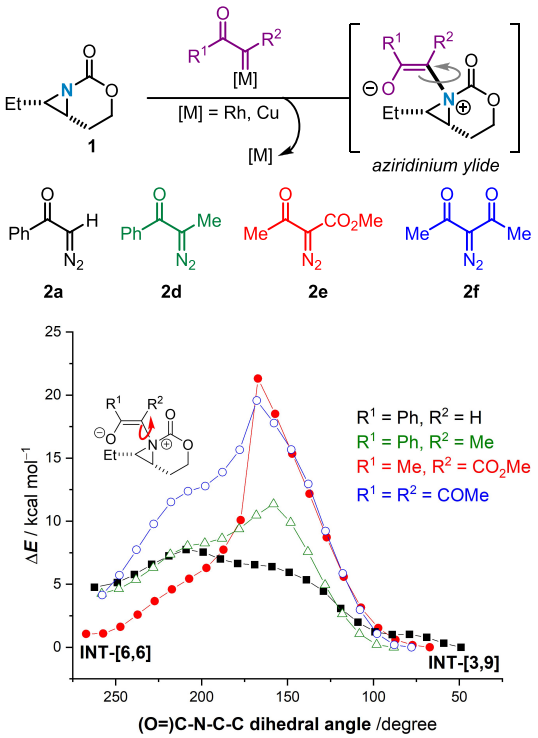

Figure 2. Computed barriers for C–N bond rotation in aziridinium ylides from diverse carbene precursors.

To test this hypothesis, aziridine **1** was treated with methylacetoacetate-derived **2e** and catalytic $Rh_2(OAc)_4$ under optimized conditions (Scheme 4A, see the Supporting Information for details). The dehydromorpholine **4e** was obtained in a 38% yield (48% by NMR), accompanied by the corresponding cheletropic extrusion product **5e** (42% by NMR). Interestingly, no competing [3,9]-aziridine **3e** was observed in the crude mixture. Computational analysis of this reaction (Scheme 4B,D) revealed that the O···C(=O) distance is much longer for **INT6** (3.085 Å) than for **INT1** (2.530 Å), a distance close to the limit of the sum of the van der Waals radii (3.22 Å). The longer distance is presumably required to accommodate the second C=O from the acceptor–acceptor carbene. This is reflected in the low computed stabilization energy (ΔE^2 (LP(O)→π*(C=O)) = −0.50 kcal/mol), which can be considered negligible. This effectively prevents formation of the undesired NCI; as a result, **INT6** and **INT5** are nearly degenerate ($\Delta\Delta G$ of ∼1 kcal/mol), a markedly different scenario from that involving **INT1**/**INT2** ylides (Figure 1A, see above). Although these computational data present a reasonable scenario for the 1:1 product mixture, we were puzzled why no **3e** was observed, considering that the predicted energy barrier is only 5.3 kcal/mol compared to 15.6 kcal/mol for **5e** (Scheme 4D). A variety of potential pathways were considered. One possibility invoked a retro-hetero-Diels–Alder reaction of **4e** to give **5e**; however, re-exposing **4e** under the standard reaction conditions (Scheme 4C) gave only recovered **4e**. Alternatively, **5e** might arise from a retro-hetero-Diels–Alder reaction of a product formed by the attack of the ester carbonyl on the aziridinium ylide by delocalization of the negative charge in **INT6**. However, computational analysis argues against this pathway, as it shows an energy barrier of 18.9 kcal/mol (see Figure S15 in the Supporting Information).

To experimentally investigate the origin of **5e**, NMR time course data were collected to identify long-lived reaction intermediates or other products not observed in the final crude mixture. The data (Figure 3) showed a consistent increase in the product **4e** over the 4 h reaction period. Interestingly, a small amount of **3e** was noted, which increased from 1 to 2 h and then decreased from 2 to 4 h, at which time the cheletropic extrusion product **5e** was observed. The 2 h reaction aliquot was further analyzed by 1D TOCSY (see Figure S9 in the Supporting Information), which revealed a unique spin system corresponding to **3e**. These data are the first experimental evidence supporting the conclusion that the reaction is under thermodynamic control (see above), where the [3,9]-aziridine **3e** gives rise to **5e**. This result is further supported by the computational data, which show that the formation of **3e** from **INT-6** is reversible in view of the low computed reaction and barrier energies (1.6 and 8.0 kcal/mol, respectively, see Scheme 4D).

https://doi.org/10.1021/acscatal.1c05413
ACS Catal. 2022, 12, 1572–1580

Scheme 4. (A–D) Competing Cheletropic Extrusion/Ring Expansion to Dehydromorpholines[a]

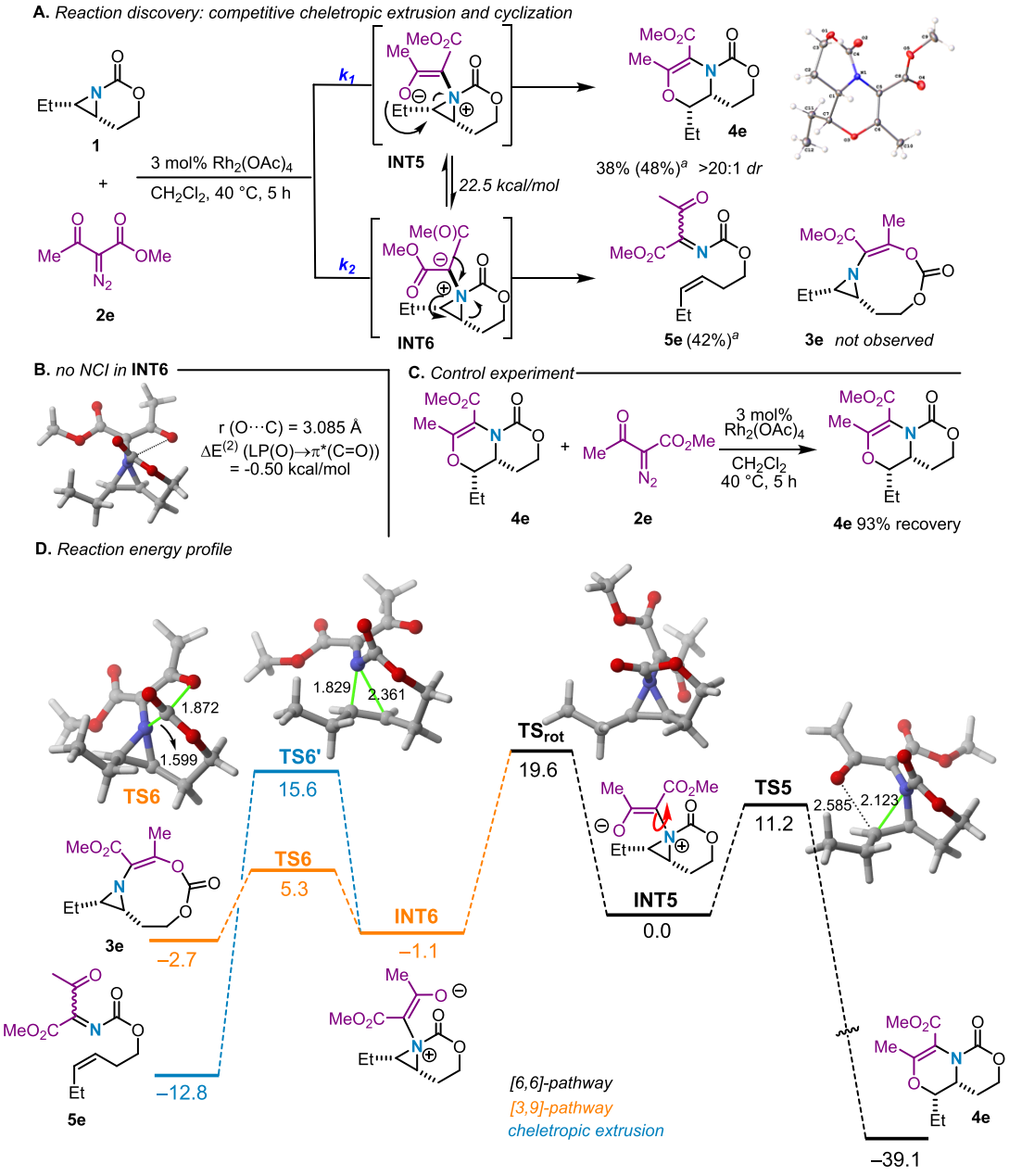

[a]See the caption of Figure 1 for computational details.

Our combined computational and experimental evidence suggests that divergent reactivity to give a ∼1:1 mixture of **4e** and **5e** is due to the non-Curtin–Hammett kinetic formation of aziridinium ylide conformers **INT5** and **INT6** (Scheme 4A). **INT5** contains a *syn*-relationship between the enolate of the methyl ketone and the external aziridine C–N bond, which represents the correct geometry for dehydromorpholine formation. The other potential aziridinium ylide **INT6** does not display the correct orientation and thus initially forms **3e**, which is ultimately converted to **5e**.

Our attempts to use nonsymmetric acceptor–acceptor diazo carbene precursors to form dehydromorpholines highlighted the importance of steric effects, rotational barriers around the C–N bond of the aziridinium ylide, and NCIs in determining the reaction outcome. Symmetric diketone-containing carbene precursors, such as **2f** (Scheme 5A), mitigated these complications by yielding only a single ylide intermediate that engages in nucleophilic ring opening of the aziridinium ylide to form the dehydromorpholine. A series of *cis*-substituted aziridines bearing linear alkyl chains, including a primary alkyl chloride, furnished **4f** and **12f–14f** as the sole products in moderate yields and high *dr* of >20:1. Isopropyl-substituted aziridine **14** was tolerated to furnish **14f**, albeit in a moderate yield, indicating the sensitivity of the reaction to steric effects. Small amounts of the cheletropic extrusion product (∼8%) were also observed in reactions of branched aziridines. Enantioenriched benzyl-substituted aziridine (*S*,*R*)-**15**, obtained in 94% *ee*, was subjected to the reaction conditions; the product **15f** was obtained in a 39% yield and an excellent >20:1 *dr*. Importantly, the 97% *ee* of **15f** (Scheme 5B) highlighted our ability to effectively transfer stereochemical information from the aziridine into the products to

https://doi.org/10.1021/acscatal.1c05413
ACS Catal. 2022, 12, 1572–1580

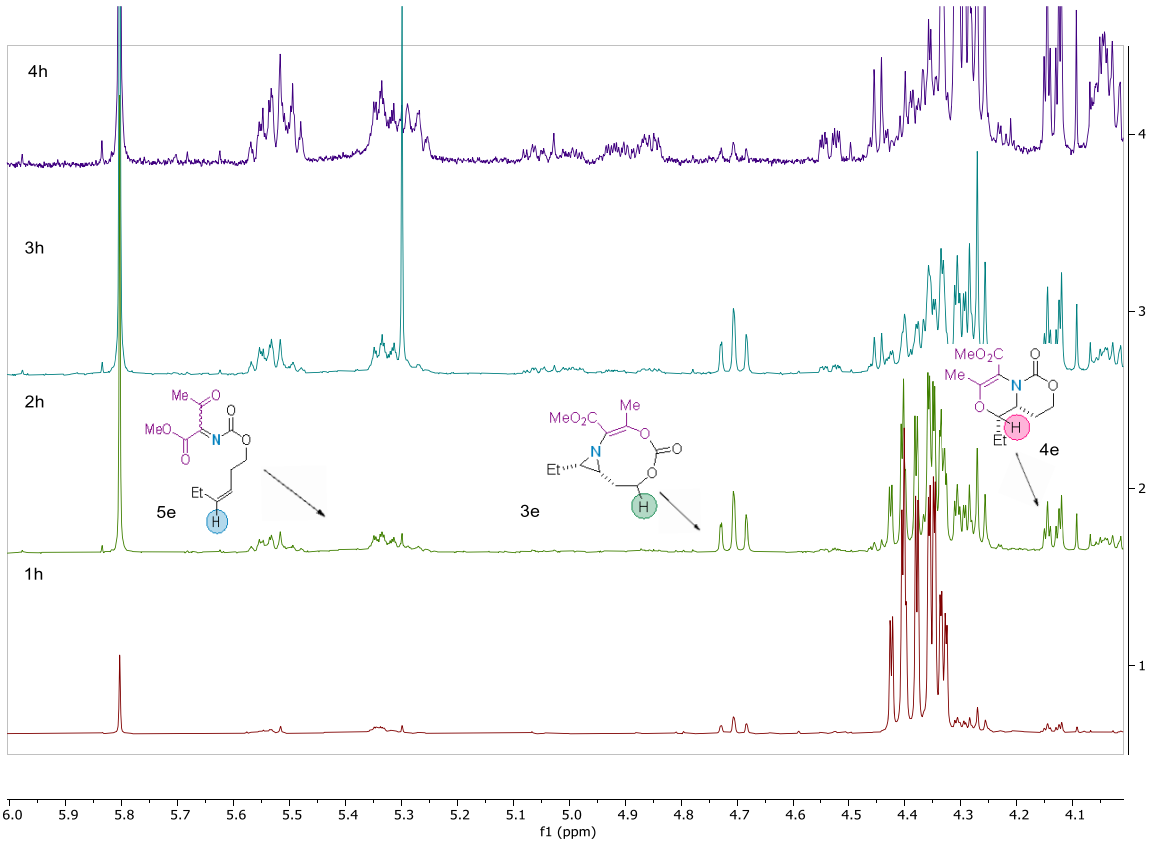

Figure 3. ^{1}H NMR time course data for the reaction of **1** and **2e**.

Scheme 5. (A−C) Dehydromorpholine Formation from Symmetric Carbene Precursors

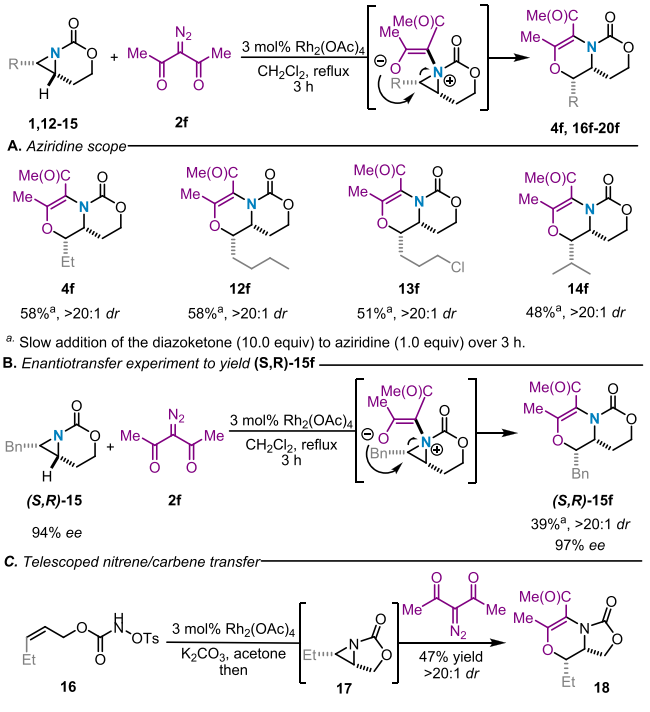

furnish enantioenriched *N*-heterocycles. This experimental result also excludes the possibility of a [4+2] hetero-Diels−Alder reaction being the operative mechanism that leads to the dehydromorpholine products **4f** and **12f−15f** (Scheme 5A,B).

This chemistry was not restricted to aziridines bearing a 6-membered bicyclic tether; a [3,5]-bicyclic aziridine **17** was capable of yielding the substituted dehydromorpholine **18** (Scheme 5C). A nice feature of this chemistry was the ability to carry out the reaction in a telescoped fashion directly from the preoxidized nitrene precursor **16** to deliver **18** in a 47% yield and >20:1 *dr* over both the aziridination and the ring expansion steps. Expansion of the telescoped reaction to more sterically demanding symmetric and unsymmetric carbene precursors with **1** proved challenging, highlighting the sensitivity of this transformation to sterics (see the Supporting Information for further details). Efforts are ongoing to address this limitation.

CONCLUSIONS

In conclusion, we have demonstrated a new method for the synthesis of highly substituted dehydromorpholines through the intermediacy of aziridinium ylides. The development of this chemistry has enabled the extension of aziridinium ylide chemistry to the concomitant formation of both a C−N and a C−O bond in a manner that preserves stereochemical information embedded in the substrate aziridine. In addition, we have uncovered several key insights that describe the importance of steric effects, rotational barriers around the C−N bond of the aziridinium ylide, and NCIs on the ultimate reaction outcome. These critical insights will assist in the further development of this chemistry to generate novel and complex *N*-heterocycles that will further expand the complex amine chemical space.

https://doi.org/10.1021/acscatal.1c05413
ACS Catal. 2022, 12, 1572−1580

■ ASSOCIATED CONTENT

Supporting Information

The Supporting Information is available free of charge at https://pubs.acs.org/doi/10.1021/acscatal.1c05413.

Experimental procedures, computational details, and characterization data for all new compounds (PDF)

X-ray crystallographic information for **3a** (CDCC Deposition Number 2124058) and **4e** (2124059) (CIF) (CIF)

■ AUTHOR INFORMATION

Corresponding Authors

Israel Fernández − *Departamento de Química Orgánica I and Centro de Innovación en Química Avanzada (ORFEO-CINQA), Facultad de Ciencias Químicas, Universidad Complutense de Madrid, Madrid 28040, Spain;* orcid.org/0000-0002-0186-9774; Email: israel@quim.ucm.es

Jennifer M. Schomaker − *Department of Chemistry, University of Wisconsin, Madison, Wisconsin 53706, United States;* orcid.org/0000-0003-1329-950X; Email: schomakerj@chem.wisc.edu

Authors

Kate A. Nicastri − *Department of Chemistry, University of Wisconsin, Madison, Wisconsin 53706, United States;* orcid.org/0000-0003-4960-0608

Soren A. Zappia − *Department of Chemistry, University of Wisconsin, Madison, Wisconsin 53706, United States*

Jared C. Pratt − *Department of Chemistry, University of Wisconsin, Madison, Wisconsin 53706, United States*

Julia M. Duncan − *Department of Chemistry, University of Wisconsin, Madison, Wisconsin 53706, United States*

Ilia A. Guzei − *Department of Chemistry, University of Wisconsin, Madison, Wisconsin 53706, United States;* orcid.org/0000-0003-1976-7386

Complete contact information is available at: https://pubs.acs.org/10.1021/acscatal.1c05413

Author Contributions

The manuscript was written through contributions of all authors. All authors have given approval to the final version of the manuscript.

Funding

J.M.S. acknowledges NIH 1R01GM132300-01 for support of this work. The NMR facilities at UW-Madison are funded by the National Science Foundation (NSF; CHE-9208463 and CHE-9629688) and the National Institutes of Health (NIH; RR08389-01). The Q-Exactive mass spectrometer was acquired from an NIH-S10 award (NIH-1S10OD020022-1). The Bruker D8 VENTURE Photon III X-ray diffractometer was partially funded by an NSF Award #CHE-1919350 to the UW-Madison Department of Chemistry. The Bruker Quazar APEX2 was purchased by UW-Madison Department of Chemistry with a portion of a generous gift from Paul J. and Margaret M. Bender. I.F. acknowledges financial support from the Spanish MCIN/AEI/10.13039/501100011033 (Grants PID2019-106184GB-I00 and RED2018-102387-T).

Notes

The authors declare no competing financial interest.

■ ACKNOWLEDGMENTS

Dr. Charlie Fry and Dr. Heike Hoffstetter of the University of Wisconsin-Madison are thanked for assistance with NMR spectroscopy, while Dr. Martha Vestling of UW-Madison is thanked for her assistance with collecting MS data. Amelia M. Wheaton is thanked for help with processing X-ray crystallographic data. Professor Robert Bergman of the University of California-Berkeley is thanked for helpful comments during the preparation of this manuscript.

■ ABBREVIATIONS

dr, diastereomeric ratio; ee, enantiomeric excess; INT, intermediate; NCI, noncovalent interaction; DFT, density functional theory; VT, variable temperature; LP, lone pair; SOPT, second-order perturbation theory; NBO, natural bond orbital; TOCSY, total correlation spectroscopy

■ REFERENCES

(1) Dequina, H. J.; Nicastri, K. A.; Schomaker, J. M. Chapter One - Additions of N, O, and S Heteroatoms to Metal-Supported Carbenes: Mechanism and Synthetic Applications in Modern Organic Chemistry. In *Advances in Organometallic Chemistry*; Pérez, P. J., Ed.; Academic Press: 2021, Vol. *76*, pp. 1−100.

(2) Doyle, M. P. 5.2 - Transition Metal Carbene Complexes: Diazodecomposition, Ylide, and Insertion. In *Comprehensive Organometallic Chemistry II*; Abel, E. W., Stone, F. G. A., Wilkinson, G., Eds.; Elsevier: Oxford, 1995, pp. 421−468.

(3) Gillingham, D.; Fei, N. Catalytic X−H Insertion Reactions Based on Carbenoids. *Chem. Soc. Rev.* **2013**, *42*, 4918−4931.

(4) Jana, S.; Guo, Y.; Koenigs, R. M. Recent Perspectives on Rearrangement Reactions of Ylides via Carbene Transfer Reactions. *Chem. − Eur. J.* **2021**, *27*, 1270−1281.

(5) Sweeney, J. B. Sigmatropic Rearrangements of 'Onium' Ylids. *Chem. Soc. Rev.* **2009**, *38*, 1027−1038.

(6) (a) Kaiser, D.; Klose, I.; Oost, R.; Neuhaus, J.; Maulide, N. Bond-Forming and -Breaking Reactions at Sulfur(IV): Sulfoxides, Sulfonium Salts, Sulfur Ylides, and Sulfinate Salts. *Chem. Rev.* **2019**, *119*, 8701−8780. (b) Zhang, Y.; Wang, J. Catalytic [2,3]-Sigmatropic Rearrangement of Sulfur Ylide Derived from Metal Carbene. *Coord. Chem. Rev.* **2010**, *254*, 941−953. (c) Lakeev, S. N.; Maydanova, I. O.; Galin, F. Z.; Tolstikov, G. A. Sulfur Ylides in the Synthesis of Heterocyclic and Carbocyclic Compounds. *Russ. Chem. Rev.* **2001**, *70*, 655−672. (d) Magdesieva, N. N.; Sergeeva, T. A. Use of Sulfonium Ylides in the Synthesis of Heterocyclic Systems (Review). *Chem. Heterocycl. Compd.* **1990**, *26*, 123−145.

(7) Murphy, G. K.; West, F. G. Oxonium Ylide Rearrangements in Synthesis. In *Molecular Rearrangements in Organic Synthesis*; John Wiley & Sons, Ltd, 2015, pp. 497−538.

(8) (a) Roiser, L.; Zielke, K.; Waser, M. Ammonium Ylide Mediated Cyclization Reactions. *Asian J. Org. Chem.* **2018**, *7*, 852−864. (b) Vanecko, J. A.; Wan, H.; West, F. G. Recent Advances in the Stevens Rearrangement of Ammonium Ylides. Application to the Synthesis of Alkaloid Natural Products. *Tetrahedron* **2006**, *62*, 1043−1062.

(9) Sheng, Z.; Zhang, Z.; Chu, C.; Zhang, Y.; Wang, J. Transition Metal-Catalyzed [2,3]-Sigmatropic Rearrangements of Ylides: An Update of the Most Recent Advances. *Tetrahedron* **2017**, *73*, 4011−4022.

(10) (a) Dequina, H. J.; Schomaker, J. M. Aziridinium Ylides: Underused Intermediates for Complex Amine Synthesis. *Trends Chem.* **2020**, *2*, 874−887. (b) Ranjith, J.; Ha, H.-J. Synthetic Applications of Aziridinium Ions. *Molecules* **2021**, *26*, 1774.

(11) (a) Gironda-Martínez, A.; Donckele, E. J.; Samain, F.; Neri, D. DNA-Encoded Chemical Libraries: A Comprehensive Review with Succesful Stories and Future Challenges. *ACS Pharmacol. Transl. Sci.* **2021**, *4*, 1265−1279. (b) Kleiner, R. E.; Dumelin, C. E.; Liu, D. R. Small-Molecule Discovery from DNA-Encoded Chemical Libraries.

Chem. Soc. Rev. **2011**, *40*, 5707−5717. (c) Martín, A.; Nicolaou, C. A.; Toledo, M. A. Navigating the DNA Encoded Libraries Chemical Space. *Commun. Chem.* **2020**, *3*, 127.
(12) (a) de Loera, D.; Liu, F.; Houk, K. N.; Garcia-Garibay, M. A. Aziridine Nitrogen Inversion by Dynamic NMR: Activation Parameters in a Fused Bicyclic Structure. *J. Org. Chem.* **2013**, *78*, 11623−11626. (b) Anet, F. A. L.; Osyany, J. M. Nuclear Magnetic Resonance Spectra and Nitrogen Inversion in 1-Acylaziridines. *J. Am. Chem. Soc.* **1967**, *89*, 352−356. (c) Bottini, A. T.; Roberts, J. D. Nuclear Magnetic Resonance Spectra. Nitrogen Inversion Rates of N-Substituted Aziridines (Ethylenimines)1. *J. Am. Chem. Soc.* **1958**, *80*, 5203−5208.
(13) Clark, J. S.; Hodgson, P. B.; Goldsmith, M. D.; Blake, A. J.; Cooke, P. A.; Street, L. J. Rearrangement of Ammonium Ylides Produced by Intramolecular Reaction of Catalytically Generated Metal Carbenoids. Part 2. Stereoselective Synthesis of Bicyclic Amines. *J. Chem. Soc., Perkin Trans. 1* **2001**, *24*, 3325−3337.
(14) Rowlands, G. J.; Kentish Barnes, W. Studies on the [2,3]-Stevens Rearrangement of Aziridinium Ions. *Tetrahedron Lett.* **2004**, *45*, 5347−5350.
(15) Hata, Y.; Watanabe, M. Fragmentation Reaction of Aziridinium Ylids. II. *Tetrahedron Lett.* **1972**, *13*, 4659−4660.
(16) (a) Ju, M.; Weatherly, C. D.; Guzei, I. A.; Schomaker, J. M. Chemo- and Enantioselective Intramolecular Silver-Catalyzed Aziridinations. *Angew. Chem., Int. Ed.* **2017**, *56*, 9944−9948. (b) Rigoli, J. W.; Weatherly, C. D.; Alderson, J. M.; Vo, B. T.; Schomaker, J. M. Tunable, Chemoselective Amination via Silver Catalysis. *J. Am. Chem. Soc.* **2013**, *135*, 17238−17241. (c) Rigoli, J. W.; Weatherly, C. D.; Vo, B. T.; Neale, S.; Meis, A. R.; Schomaker, J. M. Chemoselective Allene Aziridination via Ag(I) Catalysis. *Org. Lett.* **2013**, *15*, 290−293.
(17) Rauk, A.; Allen, L. C.; Mislow, K. Pyramidal Inversion. *Angew. Chem., Int. Ed.* **1970**, *9*, 400−414.
(18) (initial discovery) (a) Couch, J. F. Isolation of Sparteine from Lupinus Barbiger (Watson). *J. Am. Chem. Soc.* **1932**, *54*, 1691−1692. (crystal structure of sulfate salt) (b) Phillips, D. C. Crystallographic Data for Certain Alkaloids. *IV. Acta. Crystallogr.* **1954**, *7*, 603.
(19) (a) (initial discovery) Tröger, J. Ueber Einige Mittelst Nascirenden Formaldehydes Entstehende Basen. *J. Prak. Chem.* **1887**, *36*, 225−245. (structural elucidation) (b) Larson, S. B.; Wilcox, C. S. Structure of 5,11-Methano-2,8-Dimethyl-5,6,11,12-Tetrahydrodibenzo[*b*,*f*][1,5]Diazocine (Tröger's Base) at 163 K. *Acta Crystallogr., Sect. C: Cryst. Struct. Commun.* **1986**, *42*, 224−227.
(20) (a) Schmid, S. C.; Guzei, I. A.; Schomaker, J. M. A Stereoselective [3+1] Ring Expansion for the Synthesis of Highly Substituted Methylene Azetidines. *Angew. Chem., Int. Ed.* **2017**, *56*, 12229−12233. (b) Schmid, S. C.; Guzei, I. A.; Fernández, I.; Schomaker, J. M. Ring Expansion of Bicyclic Methyleneaziridines via Concerted, Near-Barrierless [2,3]-Stevens Rearrangements of Aziridinium Ylides. *ACS Catal.* **2018**, *8*, 7907−7914.
(21) Eshon, J.; Nicastri, K. A.; Schmid, S. C.; Raskopf, W. T.; Guzei, I. A.; Fernández, I.; Schomaker, J. M. Intermolecular [3+3] Ring Expansion of Aziridines to Dehydropiperi-dines through the Intermediacy of Aziridinium Ylides. *Nat. Commun.* **2020**, *11*, 1273.
(22) Wang, L.; Liu, Q.-B.; Wang, D.-S.; Li, X.; Han, X.-W.; Xiao, W.-J.; Zhou, Y.-G. Tandem Ring-Opening/Closing Reactions of N-Ts Aziridines and Aryl Propargyl Alcohols Promoted by t-BuOK. *Org. Lett.* **2009**, *11*, 1119−1122.
(23) Zhang, S.; Shan, C.; Zhang, S.; Yuan, L.; Wang, J.; Tung, C.-H.; Xing, L.-B.; Xu, Z. Breaking Aziridines to Construct Morpholines with a Gold(I)-Catalyzed Tandem Ring-Opening and Cycloisomerization Reaction. *Org. Biomol. Chem.* **2016**, *14*, 10973−10980.
(24) Fang, S.; Zhao, Y.; Li, H.; Zheng, Y.; Lian, P.; Wan, X. [3 + 3]-Cycloaddition of α-Diazocarbonyl Compounds and N-Tosylaziridines: Synthesis of Polysubstituted 2H-1,4-Oxazines through Synergetic Catalysis of AgOTf/$Cu(OAc)_2$. *Org. Lett.* **2019**, *21*, 2356−2359.

https://doi.org/10.1021/acscatal.1c05413
ACS Catal. 2022, 12, 1572−1580